Investigation of Finite Element Methods for a 4D Hybrid Plasma Model

Florian Holderied

Master's Colloquium, 15.03.2019

1. Motivation

Self-consistent description of energetic particle (EP) interaction with a thermal bulk plasma for long times

In Tokamaks[1]:

- 3.5 MeV α-particles in a burning plasma

$$
\begin{aligned}
&{}^3_1\mathrm{T} + {}^2_1\mathrm{D} \;\rightarrow\; {}^4_2\alpha\,(3.5\,\mathrm{MeV}) + {}^0_1\mathrm{n}\,(14.1\,\mathrm{MeV}),\\
&v_\alpha \approx v_{\mathrm{Alfvén}} \sim 10^7\ \mathrm{m/s}
\end{aligned}
$$

- Additional fast particles coming from heating devices such as
  - neutral beam injection (NBI)
  - ion/electron resonance heating (ICRH/ECRH)

In space[2]:

- Energetic electrons in planetary magnetospheres (*Chorus waves*)

[1]Chen et al., Rev. Mod. Phys. **88**, 015008 (2016)

[2]Tao, J. Geophys. Res. **119**, 3362-3372 (2014)

1. Motivation

Self-consistent description of energetic particle (EP) interaction with a thermal bulk plasma for long times

- **Hybrid models**: Fluid models for bulk plasma and kinetic description for energetic particles (accuracy vs. computational costs)

- **FEEC[3]/GEMPIC[4]**: Finite element exterior calculus/Geometric electromagnetic particle-in-cell methods

  $\rightarrow$ algorithms with good stability and conservation properties

Aim of this work: Application of standard FEM/PIC and FEEC/GEMPIC on a 4d hybrid plasma model, implementation in Python, verification of codes and comparison of results

[3] Arnold et al., Acta Numerica **15**, 1-155 (2006)

[4] Kraus et al., J. Plasma Phys. **83**, 905830401 (2017)

Outline

1. Motivation
2. Current coupling electron hybrid model
3. Numerical treatment and results
   - Standard finite elements/PIC
   - Finite element exterior calculus/GEMPIC
4. Summary

Outline

1. Motivation
2. Current coupling electron hybrid model
3. Numerical treatment and results
   - Standard finite elements/PIC
   - Finite element exterior calculus/GEMPIC
4. Summary

2. Current coupling electron hybrid model

Assumptions:

- High-frequency plasma model $\longrightarrow$ wave frequencies $\omega \approx \Omega_{\mathrm{ce}}$
- Two electron species: 1. Cold fluid electrons (c) $v_{\mathrm{th,c}} \ll v_{\mathrm{ph}}$

  2. Energetic kinetic electrons (h) $v_{\mathrm{th,h}} \approx v_{\mathrm{ph}}$
- Linearized fluid and field equations

  $n_{\mathrm{c}} = n_{\mathrm{c0}} + \tilde{n}_{\mathrm{c}}$, $\mathbf{B} = \mathbf{B}_0 + \tilde{\mathbf{B}}$, $\mathbf{E} = \tilde{\mathbf{E}}$, $\mathbf{u}_{\mathrm{c}} = \tilde{\mathbf{u}}_{\mathrm{c}} \quad \Rightarrow \quad \tilde{\mathbf{j}}_{\mathrm{c}} \approx q_{\mathrm{e}} n_{\mathrm{c0}} \tilde{\mathbf{u}}_{\mathrm{c}}$

Assumptions:

- High-frequency plasma model $\longrightarrow$ wave frequencies $\omega \approx \Omega_{\mathsf{ce}}$
- Two electron species:
  1. Cold fluid electrons (c) $\quad v_{\mathsf{th,c}} \ll v_{\mathsf{ph}}$
  2. Energetic kinetic electrons (h) $\quad v_{\mathsf{th,h}} \approx v_{\mathsf{ph}}$
- Linearized fluid and field equations

$$n_{\mathsf{c}} = n_{\mathsf{c0}} + \tilde{n}_{\mathsf{c}},\ \mathbf{B} = \mathbf{B}_0 + \tilde{\mathbf{B}},\ \mathbf{E} = \tilde{\mathbf{E}},\ \mathbf{u}_{\mathrm{c}} = \tilde{\mathbf{u}}_{\mathrm{c}} \quad \Rightarrow \quad \tilde{\mathbf{j}}_{\mathsf{c}} \approx q_{\mathrm{e}} n_{\mathsf{c0}} \tilde{\mathbf{u}}_{\mathrm{c}}$$

$$\frac{\partial \tilde{\mathbf{j}}_{\mathsf{c}}}{\partial t} = \epsilon_0 \Omega_{\mathsf{pe}}^2(\mathbf{x}) \tilde{\mathbf{E}} + \tilde{\mathbf{j}}_{\mathsf{c}} \times \boldsymbol{\Omega}_{\mathsf{ce}}(\mathbf{x}) \qquad \text{(Lin. momentum balance)}$$

$$\frac{\partial \tilde{\mathbf{B}}}{\partial t} = -\nabla \times \tilde{\mathbf{E}} \qquad \text{(Faraday)}$$

$$\frac{1}{c^2} \frac{\partial \tilde{\mathbf{E}}}{\partial t} = \nabla \times \tilde{\mathbf{B}} - \mu_0 (\tilde{\mathbf{j}}_{\mathsf{c}} + \tilde{\mathbf{j}}_{\mathsf{h}}) \qquad \text{(Ampère)}$$

$$\frac{\partial f_{\mathsf{h}}}{\partial t} + \mathbf{v} \cdot \nabla f_{\mathsf{h}} + \frac{q_{\mathsf{e}}}{m_{\mathsf{e}}} (\mathbf{E} + \mathbf{v} \times \mathbf{B}) \cdot \nabla_{\mathbf{v}} f_{\mathsf{h}} = 0 \qquad \text{(Vlasov)}$$

2. Current coupling electron hybrid model

Dispersion relation for ...

- ... a homogeneous plasma $n_{c0} = const.$ $\quad\Rightarrow\quad \Omega_{pe} = const.$
- ... a uniform background field $\mathbf{B}_0 = B_0\mathbf{e}_z$ $\quad\Rightarrow\quad |\mathbf{\Omega}_{ce}| = const.$
- ... parallel wave propagation $\mathbf{k} \parallel \mathbf{B}_0$ $\quad\Rightarrow\quad \nabla = \mathbf{e}_z\partial_z$
- ... a uniform equilibrium energetic electron distribution

$$f_h(z,\mathbf{v},t) = f_h^0(\mathbf{v}) + \tilde{f}_h(z,\mathbf{v},t), \quad \tilde{f}_h \ll f_h^0$$

Solution: Plane wave ansatz for all perturbed quantities, e.g.

$$\tilde{f}_h(z,\mathbf{v},t) = \hat{f}_h(\mathbf{v})\exp\left[i(kz-\omega t)\right][5]$$
$$\tilde{B}(z,t) = \hat{B}\exp\left[i(kz-\omega t)\right]$$

[5] Brambilla, Kinetic Theory of Plasma Waves, Oxford University Press, 1998

2. Current coupling electron hybrid model

3 linear independent solutions:

- 1 electrostatic $\tilde{\mathbf{E}} \parallel \mathbf{k}$, $\tilde{\mathbf{B}} = 0$ $\rightarrow$ Plasma oscillations (Landau damping)
- 2 electromagnetic $\tilde{\mathbf{E}}, \tilde{\mathbf{B}} \perp \mathbf{k}$ $\rightarrow$ Circularly polarized waves (R/L)

Dispersion relation for electromagnetic perturbations:

$$D_{\mathrm{R/L}}(k,\omega) = D_{\mathrm{R/L}}^{\mathrm{cold}}(k,\omega) + \nu_{\mathrm{h}} \frac{\Omega_{\mathrm{pe}}^2}{\omega} \int \mathrm{d}^3\mathbf{v} \, \frac{v_\perp}{2} \frac{\hat{G} F_{\mathrm{h}}^0(v_\parallel, v_\perp)}{\omega \pm \Omega_{\mathrm{ce}} - k v_\parallel} \overset{!}{=} 0$$

$$D_{\mathrm{R/L}}^{\mathrm{cold}}(k,\omega) = 1 - \frac{c^2k^2}{\omega^2} - \frac{\Omega_{\mathrm{pe}}^2}{\omega(\omega \pm \Omega_{\mathrm{ce}})}, \quad \nu_{\mathrm{h}} = n_{\mathrm{h0}}/n_{\mathrm{c0}} \ll 1$$

$\Rightarrow$ Wave-particle interaction due to energetic electrons with $k v_\parallel \mp \Omega_{\mathrm{ce}} = \omega$

2. Current coupling electron hybrid model

Example: anisotropic Maxwellian with respect to $\mathbf{B}_0 = B_0\mathbf{e}_z$

$$F_{\mathrm{h}}^0(v_\parallel, v_\perp) = \frac{1}{(2\pi)^{3/2} v_{\mathrm{th}\parallel} v_{\mathrm{th}\perp}^2} \exp\left(-\frac{v_\parallel^2}{2v_{\mathrm{th}\parallel}^2} - \frac{v_\perp^2}{2v_{\mathrm{th}\perp}^2}\right)$$

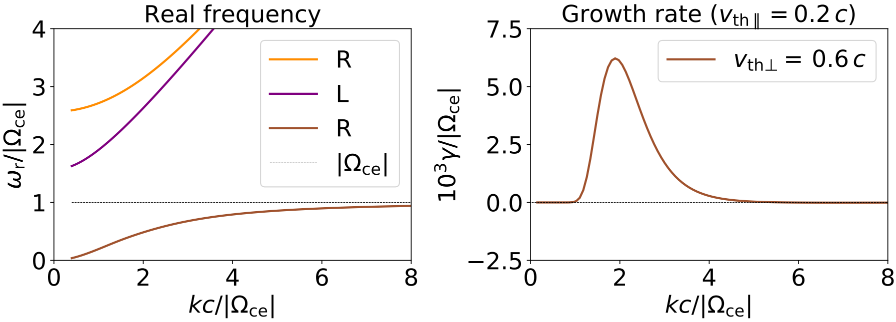

Figure: Solutions of the hybrid dispersion relation for $\nu_{\mathrm{h}} = 0.5\,\%$, $\Omega_{\mathrm{pe}} = 2|\Omega_{\mathrm{ce}}|$.

2. Current coupling electron hybrid model

Example: anisotropic Maxwellian with respect to $\mathbf{B}_0 = B_0\mathbf{e}_z$

$$F_\mathrm{h}^0(v_\|, v_\perp) = \frac{1}{(2\pi)^{3/2} v_{\mathrm{th}\|} v_{\mathrm{th}\perp}^2} \exp\left(-\frac{v_\|^2}{2v_{\mathrm{th}\|}^2} - \frac{v_\perp^2}{2v_{\mathrm{th}\perp}^2}\right)$$

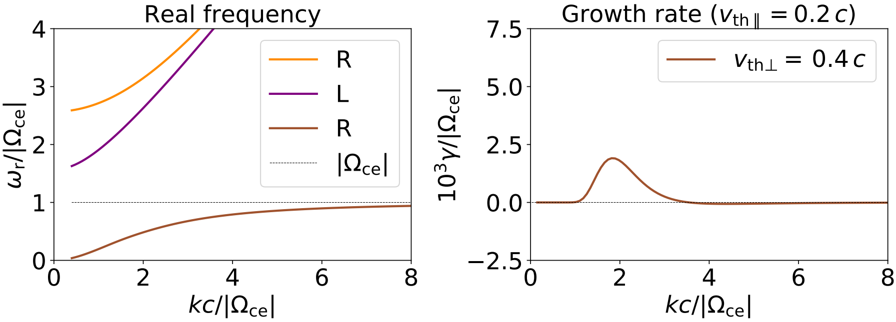

Figure: Solutions of the hybrid dispersion relation for $\nu_\mathrm{h} = 0.5\,\%$, $\Omega_\mathrm{pe} = 2|\Omega_\mathrm{ce}|$.

Example: anisotropic Maxwellian with respect to $\mathbf{B}_0 = B_0\mathbf{e}_z$

$$F_{\mathrm{h}}^0(v_\parallel, v_\perp) = \frac{1}{(2\pi)^{3/2} v_{\mathrm{th}\parallel} v_{\mathrm{th}\perp}^2} \exp\left(-\frac{v_\parallel^2}{2v_{\mathrm{th}\parallel}^2} - \frac{v_\perp^2}{2v_{\mathrm{th}\perp}^2} \right)$$

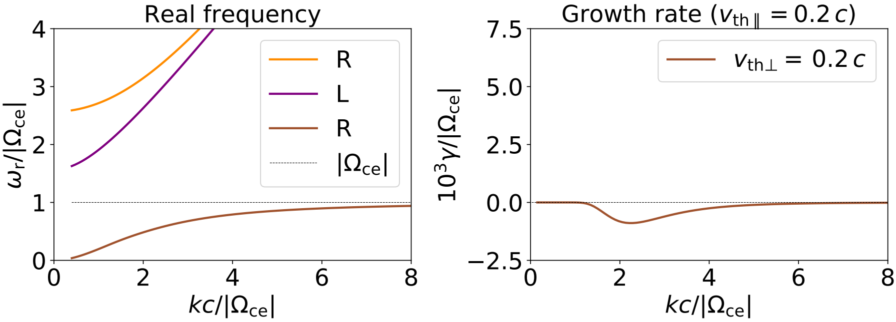

Figure: Solutions of the hybrid dispersion relation for $\nu_{\mathrm{h}} = 0.5\,\%$, $\Omega_{\mathrm{pe}} = 2|\Omega_{\mathrm{ce}}|$.

Example: anisotropic Maxwellian with respect to $\mathbf{B}_0 = B_0 \mathbf{e}_z$

$$F_{\mathrm{h}}^0(v_\parallel, v_\perp) = \frac{1}{(2\pi)^{3/2} v_{\mathrm{th}\parallel} v_{\mathrm{th}\perp}^2} \exp\left(-\frac{v_\parallel^2}{2v_{\mathrm{th}\parallel}^2} - \frac{v_\perp^2}{2v_{\mathrm{th}\perp}^2} \right)$$

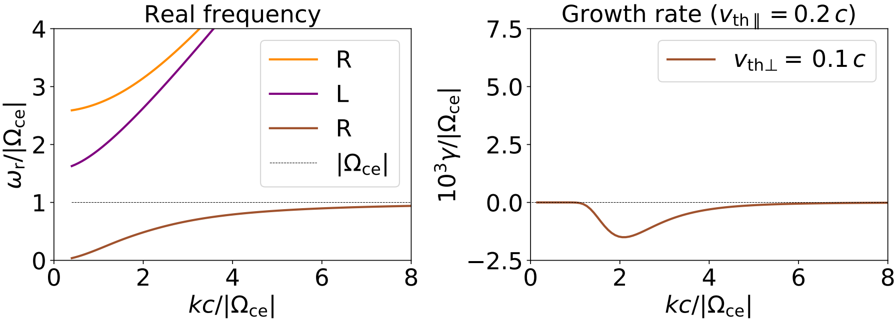

Figure: Solutions of the hybrid dispersion relation for $\nu_{\mathrm{h}} = 0.5\,\%$, $\Omega_{\mathrm{pe}} = 2|\Omega_{\mathrm{ce}}|$.

Outline

Standard finite elements/PIC

- 1d B-spline finite elements for
  - cold plasma current $\tilde{\mathbf{j}}_\mathrm{c}$
  - electromagnetic fields $\tilde{\mathbf{E}}$, $\tilde{\mathbf{B}}$

$$\Rightarrow \quad M_\mathrm{b}\frac{\mathrm{d}\mathbf{u}}{\mathrm{d}t} + \tilde{C}\mathbf{u} + \tilde{M}\mathbf{u} = \mathbf{s}, \qquad \mathbf{u} \in \mathbb{R}^{6N}$$

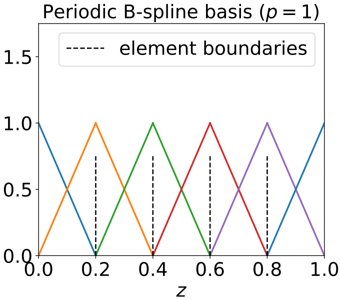

$$\text{e.g. } \tilde{B}_{xh}(z,t) = \sum_{j=1}^{N} b_{xj}(t)\varphi_j(z)$$

Standard finite elements/PIC

- 1d B-spline finite elements for
  - cold plasma current $\tilde{\mathbf{j}}_\mathrm{c}$
  - electromagnetic fields $\tilde{\mathbf{E}}$, $\tilde{\mathbf{B}}$

$$\Rightarrow \quad M_\mathrm{b}\frac{\mathrm{d}\mathbf{u}}{\mathrm{d}t} + \tilde{C}\mathbf{u} + \tilde{M}\mathbf{u} = \mathbf{s}, \qquad \mathbf{u} \in \mathbb{R}^{6N}$$

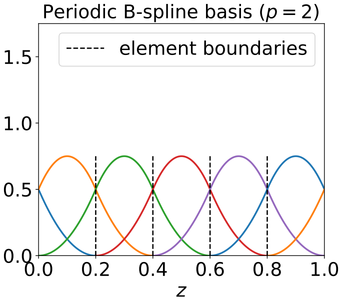

e.g. $\tilde{B}_{xh}(z,t) = \sum_{j=1}^{N} b_{xj}(t)\varphi_j(z)$

Standard finite elements/PIC

- 1d B-spline finite elements for
  - cold plasma current $\tilde{\mathbf{j}}_{\mathrm{c}}$
  - electromagnetic fields $\tilde{\mathbf{E}}$, $\tilde{\mathbf{B}}$

$$\Rightarrow \quad M_{\mathrm{b}} \frac{\mathrm{d}\mathbf{u}}{\mathrm{d}t} + \tilde{C}\mathbf{u} + \tilde{M}\mathbf{u} = \mathbf{s}, \qquad \mathbf{u} \in \mathbb{R}^{6N}$$

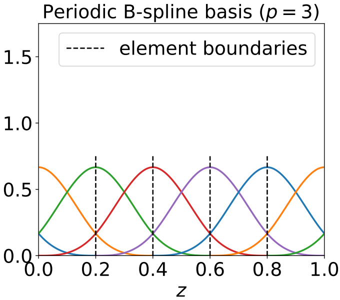

$$\text{e.g. } \tilde{B}_{xh}(z,t) = \sum_{j=1}^{N} b_{xj}(t)\varphi_j(z)$$

Standard finite elements/PIC

- 1d B-spline finite elements for
  - cold plasma current $\tilde{\mathbf{j}}_\mathrm{c}$
  - electromagnetic fields $\tilde{\mathbf{E}}$, $\tilde{\mathbf{B}}$

$$\Rightarrow \quad M_\mathrm{b}\frac{\mathrm{d}\mathbf{u}}{\mathrm{d}t} + \tilde{C}\mathbf{u} + \tilde{M}\mathbf{u} = \mathbf{s}, \qquad \mathbf{u} \in \mathbb{R}^{6N}$$

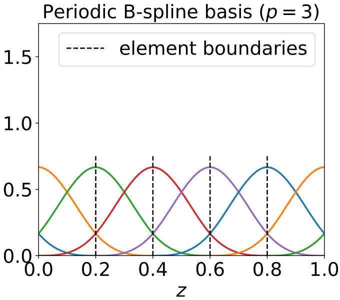

- 1d3v particle-in-cell for $\mathbf{s}$ with Boris particle pusher

$$f_\mathrm{h}(z, \mathbf{v}, t) \approx \sum_{k=1}^{N_\mathrm{p}} w_k \delta(z - z_k(t))\delta(\mathbf{v} - \mathbf{v}_k(t))$$

Standard finite elements/PIC

- 1d B-spline finite elements for
  - cold plasma current $\tilde{\mathbf{j}}_\mathrm{c}$
  - electromagnetic fields $\tilde{\mathbf{E}}$, $\tilde{\mathbf{B}}$

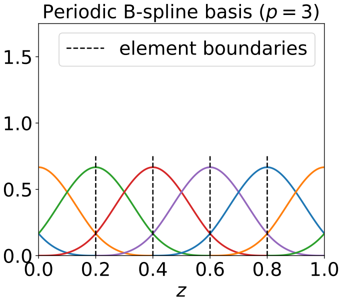

$$\Rightarrow \quad M_\mathrm{b}\frac{\mathrm{d}\mathbf{u}}{\mathrm{d}t} + \tilde{C}\mathbf{u} + \tilde{M}\mathbf{u} = \mathbf{s}, \qquad \mathbf{u} \in \mathbb{R}^{6N}$$

- 1d3v particle-in-cell for $\mathbf{s}$ with Boris particle pusher
  - without control variate: simulation of full f_h $\quad\Rightarrow\quad w_k = const.$
  - with control variate: simulation of $f_\mathrm{h} - f_\mathrm{h}^0$ $\quad\Rightarrow\quad w_k = w_k(t)$

Standard finite elements/PIC

- 1d B-spline finite elements for
  - cold plasma current $\tilde{\mathbf{j}}_c$
  - electromagnetic fields $\tilde{\mathbf{E}}$, $\tilde{\mathbf{B}}$

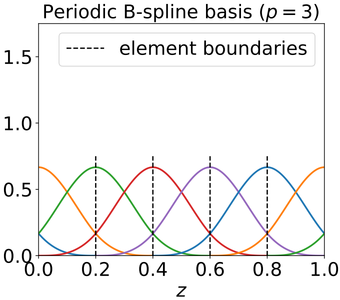

$$\Rightarrow \quad M_b \frac{d\mathbf{u}}{dt} + \tilde{C}\mathbf{u} + \tilde{M}\mathbf{u} = \mathbf{s}, \qquad \mathbf{u} \in \mathbb{R}^{6N}$$

- 1d3v particle-in-cell for $\mathbf{s}$ with Boris particle pusher
  - without control variate: simulation of full f_h $\quad \Rightarrow \quad w_k = const.$
  - with control variate: simulation of $f_h - f_h^0$ $\quad \Rightarrow \quad w_k = w_k(t)$
- 2nd order Crank-Nicolson time stepping scheme for semi-discrete system

Standard finite elements/PIC: Results

Test run: Anisotropic Maxwellian ($\nu_\mathrm{h} = 6\,\%,\ v_{\mathrm{th}\|} < v_{\mathrm{th}\perp}$) for energetic electrons and initial magnetic field perturbation $\tilde{B}_x(z, t=0) = a\sin(kz)$, **with** control variate

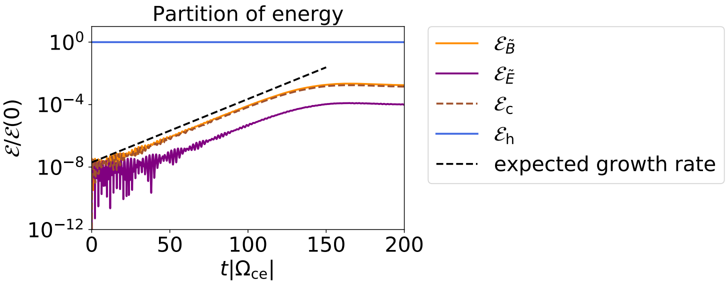

Figure: Time evolution of all energies in the system

Standard finite elements/PIC: Results

Test run: Anisotropic Maxwellian ($\nu_{\mathrm{h}} = 6\,\%$, $v_{\mathrm{th}\|} < v_{\mathrm{th}\perp}$) for energetic electrons and initial magnetic field perturbation $\tilde{B}_x(z, t = 0) = a\sin(kz)$, **with** control variate

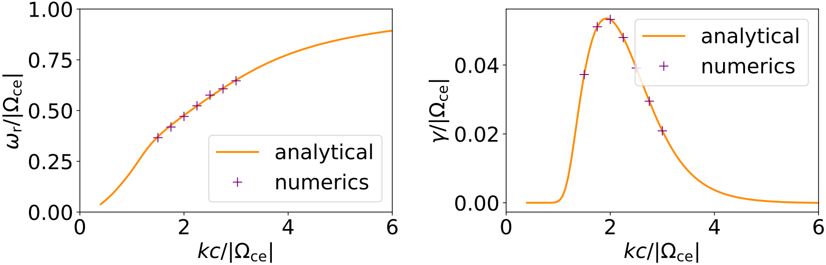

Figure: Comparison of real frequencies/growth rates obtained by numerics and analytical theory

Standard finite elements/PIC: Results

Test run: Anisotropic Maxwellian ($\nu_\mathrm{h} = 6\,\%$, $v_{\mathrm{th}\|} < v_{\mathrm{th}\perp}$) for energetic electrons and initial magnetic field perturbation $\tilde{B}_x(z, t = 0) = a\sin(kz)$, **with** control variate

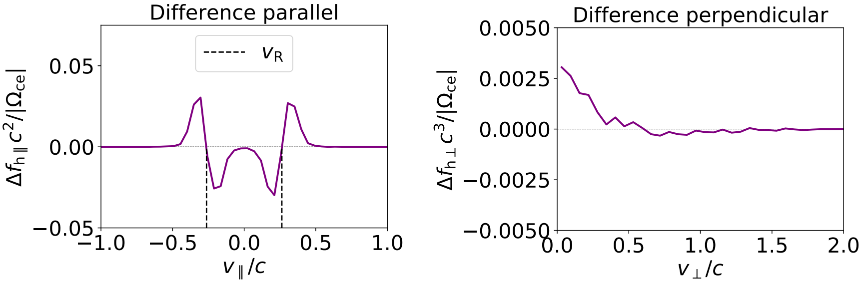

Figure: Difference between initial and final fast electron velocity distributions

Standard finite elements/PIC: Results

Test run: Anisotropic Maxwellian ($\nu_\mathrm{h} = 6\,\%$, $v_{\mathrm{th}\|} < v_{\mathrm{th}\perp}$) for energetic electrons and initial magnetic field perturbation $\tilde{B}_x(z, t = 0) = a\sin(kz)$, **with** control variate

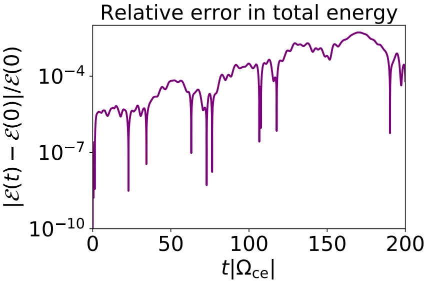

Figure: Time evolution of the error in the conservation of energy

Outline

Finite element exterior calculus (FEEC) in a nutshell

$$\begin{tikzcd}
H^1(\Omega) \arrow[r, "\mathrm{grad}"] \arrow[d, "\Pi_0"'] & H(\mathrm{curl},\Omega) \arrow[r, "\mathrm{curl}"] \arrow[d, "\Pi_1"'] & H(\mathrm{div},\Omega) \arrow[r, "\mathrm{div}"] \arrow[d, "\Pi_2"'] & L^2(\Omega) \arrow[d, "\Pi_3"'] \\
V_0 \arrow[r, "\mathrm{grad}"] & V_1 \arrow[r, "\mathrm{curl}"] & V_2 \arrow[r, "\mathrm{div}"] & V_3
\end{tikzcd}$$

Diagram is commuting: e.g. for $\Phi \in H^1(\Omega)$ we have

$$\mathrm{grad}(\Pi_0\Phi) = \Pi_1(\mathrm{grad}\Phi)$$

Idea: Not discretizing only points values (Π_0), but also edge integrals (Π_1), face integrals (Π_2) and volume integrals (Π_3)

FEEC: Simplifications in 1d

- 1d Lagrange interpolation for $\Pi_0 : H^1 \to V_0$, $(\Pi_0\Phi)(z_i) = \Phi(z_i)$
- 1d Lagrange histopolation for $\Pi_1 : L^2 \to V_1$, $\int_{z_i}^{z_{i+1}} (\Pi_1\Phi)(z)\mathrm{d}z = \int_{z_i}^{z_{i+1}} \Phi(z)\mathrm{d}z$

$$\begin{tikzcd} H^1(\Omega) \arrow[r, "\partial/\partial z"] \arrow[d, "\Pi_0"'] & L^2(\Omega) \arrow[d, "\Pi_1"] \\ V_0 \arrow[r, "\partial/\partial z"'] & V_1 \end{tikzcd}$$

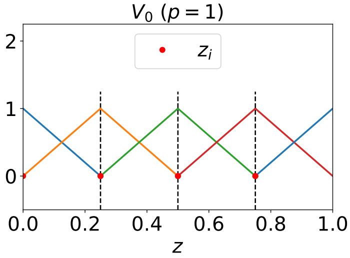

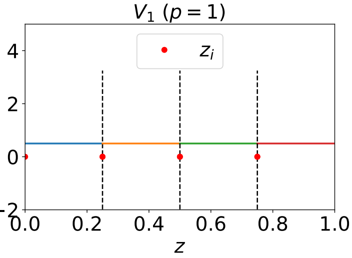

3. Numerical treatment and results

FEEC: Simplifications in 1d

- 1d Lagrange interpolation for $\Pi_0 : H^1 \to V_0$, $(\Pi_0\Phi)(z_i) = \Phi(z_i)$
- 1d Lagrange histopolation for $\Pi_1 : L^2 \to V_1$, $\int_{z_i}^{z_{i+1}} (\Pi_1\Phi)(z)\mathrm{d}z = \int_{z_i}^{z_{i+1}} \Phi(z)\mathrm{d}z$

$$
\begin{tikzcd}
H^1(\Omega) \arrow[r, "\partial/\partial z"] \arrow[d, "\Pi_0"'] & L^2(\Omega) \arrow[d, "\Pi_1"'] \\
V_0 \arrow[r, "\partial/\partial z"'] & V_1
\end{tikzcd}
$$

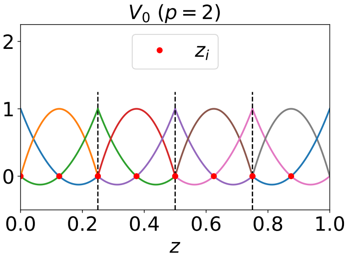

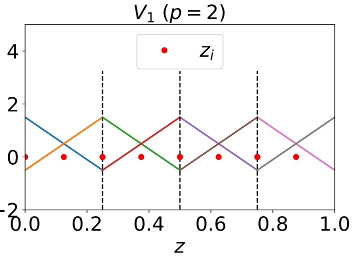

FEEC: Simplifications in 1d

- 1d Lagrange interpolation for $\Pi_0 : H^1 \to V_0$, $(\Pi_0\Phi)(z_i) = \Phi(z_i)$
- 1d Lagrange histopolation for $\Pi_1 : L^2 \to V_1$, $\int_{z_i}^{z_{i+1}}(\Pi_1\Phi)(z)\mathrm{d}z = \int_{z_i}^{z_{i+1}}\Phi(z)\mathrm{d}z$

$$
\begin{tikzcd}
H^1(\Omega) \arrow[r, "\partial/\partial z"] \arrow[d, "\Pi_0"'] & L^2(\Omega) \arrow[d, "\Pi_1"'] \\
V_0 \arrow[r, "\partial/\partial z"'] & V_1
\end{tikzcd}
$$

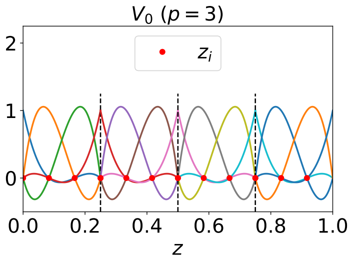

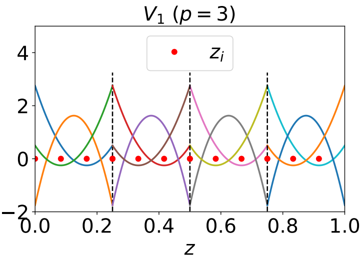

FEEC/GEMPIC: Application on hybrid model

- Choose $\tilde{E}_x$, $\tilde{E}_y$, $\tilde{j}_{cx}$, $\tilde{j}_{cy} \in H^1$ (discrete counterparts $\in V_0$)

$$\frac{\partial \tilde{\mathbf{j}}_\mathrm{c}}{\partial t} = \epsilon_0 \Omega_\mathrm{pe}^2 \tilde{\mathbf{E}} + \Omega_\mathrm{ce} \tilde{\mathbf{j}}_\mathrm{c} \times \mathbf{e}_z$$

$$\frac{1}{c^2}\frac{\partial \tilde{\mathbf{E}}}{\partial t} = \mathbf{e}_z \frac{\partial}{\partial z} \times \tilde{\mathbf{B}} - \mu_0 (\tilde{\mathbf{j}}_\mathrm{c} + \tilde{\mathbf{j}}_\mathrm{h})$$

FEEC/GEMPIC: Application on hybrid model

- Choose $\tilde{E}_x$, $\tilde{E}_y$, $\tilde{j}_{cx}$, $\tilde{j}_{cy} \in H^1$ (discrete counterparts $\in V_0$)
- Choose $\tilde{B}_x$, $\tilde{B}_y \in L^2$ (discrete counterparts $\in V_1$)
  $\Rightarrow$ integration by parts in weak formulation

$$\frac{\partial \tilde{\mathbf{B}}}{\partial t} = -\mathbf{e}_z \frac{\partial}{\partial z} \times \tilde{\mathbf{E}}$$

$$\frac{1}{c^2}\frac{\partial \tilde{\mathbf{E}}}{\partial t} = \mathbf{e}_z \frac{\partial}{\partial z} \times \tilde{\mathbf{B}} - \mu_0(\tilde{\mathbf{j}}_{\mathrm{c}} + \tilde{\mathbf{j}}_{\mathrm{h}})$$

FEEC/GEMPIC: Application on hybrid model

- Choose $\tilde{E}_x$, $\tilde{E}_y$, $\tilde{j}_{cx}$, $\tilde{j}_{cy} \in H^1$ (discrete counterparts $\in V_0$)
- Choose $\tilde{B}_x$, $\tilde{B}_y \in L^2$ (discrete counterparts $\in V_1$)
  $\Rightarrow$ integration by parts in weak formulation
- PIC for Vlasov equation

FEEC/GEMPIC: Application on hybrid model

- Choose $\tilde{E}_x$, $\tilde{E}_y$, $\tilde{j}_{\mathrm{c}x}$, $\tilde{j}_{\mathrm{c}y} \in H^1$ (discrete counterparts $\in V_0$)
- Choose $\tilde{B}_x$, $\tilde{B}_y \in L^2$ (discrete counterparts $\in V_1$)
  $\Rightarrow$ integration by parts in weak formulation
- PIC for Vlasov equation
- Semi-discrete system exhibits a non-canonical Hamiltonian structure[6]

$$\frac{\mathrm{d}\mathbf{u}}{\mathrm{d}t} = \mathbb{J}(\mathbf{u})\nabla_{\mathbf{u}} H(\mathbf{u}), \quad \mathbf{u} \in \mathbb{R}^{2N_0+2N_1+4N_\mathrm{p}}$$

$$H(\mathbf{u}) = H_E + H_B + H_\mathrm{c} + H_\mathrm{h}$$

$\Rightarrow$ **exact energy conservation!**

[6] Holderied, Possanner, Ratnani & Wang in preparation

FEEC/GEMPIC: Application on hybrid model

- Choose $\tilde{E}_x$, $\tilde{E}_y$, $\tilde{j}_{cx}$, $\tilde{j}_{cy} \in H^1$ (discrete counterparts $\in V_0$)
- Choose $\tilde{B}_x$, $\tilde{B}_y \in L^2$ (discrete counterparts $\in V_1$)
  $\Rightarrow$ integration by parts in weak formulation
- PIC for Vlasov equation
- Semi-discrete system exhibits a non-canonical Hamiltonian structure[6]

$$\frac{\mathrm{d}\mathbf{u}}{\mathrm{d}t} = \mathbb{J}(\mathbf{u})\nabla_{\mathbf{u}} H(\mathbf{u}), \quad \mathbf{u} \in \mathbb{R}^{2N_0+2N_1+4N_\mathrm{p}}$$

$$H(\mathbf{u}) = H_E + H_B + H_\mathrm{c} + H_\mathrm{h}$$

$\Rightarrow$ **exact energy conservation!**

- Poisson integrators for time integration obtained by Hamiltonian splitting

e.g. solve $\quad \frac{\mathrm{d}\mathbf{u}}{\mathrm{d}t} = \mathbb{J}(\mathbf{u})\nabla_{\mathbf{u}} H_E(\mathbf{u}) \quad \rightarrow \quad \frac{\mathrm{d}\mathbf{u}}{\mathrm{d}t} = \mathbb{J}(\mathbf{u})\nabla_{\mathbf{u}} H_B(\mathbf{u}) \quad \rightarrow \quad \dots$

[6] Holderied, Possanner, Ratnani & Wang in preparation

FEEC/GEMPIC: Results

Test run: Anisotropic Maxwellian ($\nu_\mathrm{h} = 6\%$, $v_{\mathrm{th}\|} < v_{\mathrm{th}\perp}$) for fast electrons and an initial magnetic field perturbation $\tilde{B}_x(z, t = 0) = a\sin(kz)$, **without** control variate

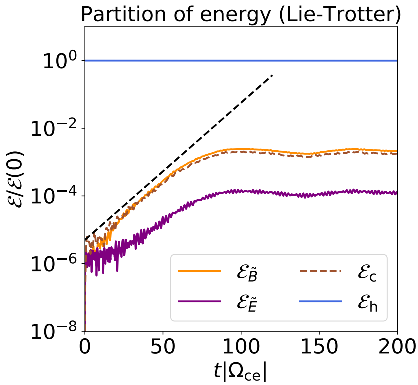

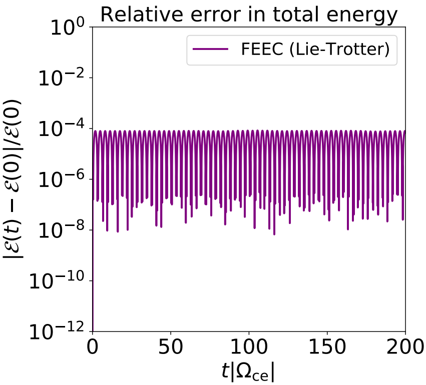

FEEC/GEMPIC: Results

Test run: Anisotropic Maxwellian ($\nu_\mathrm{h} = 6\%$, $v_{\mathrm{th}||} < v_{\mathrm{th}\perp}$) for fast electrons and an initial magnetic field perturbation $\tilde{B}_x(z, t = 0) = a \sin(kz)$, **without** control variate

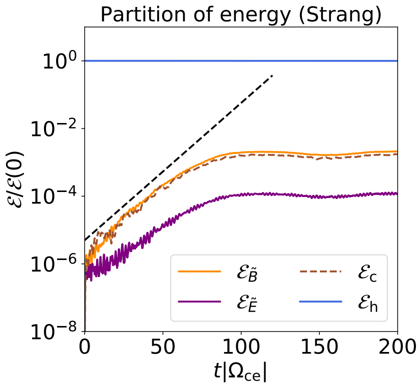

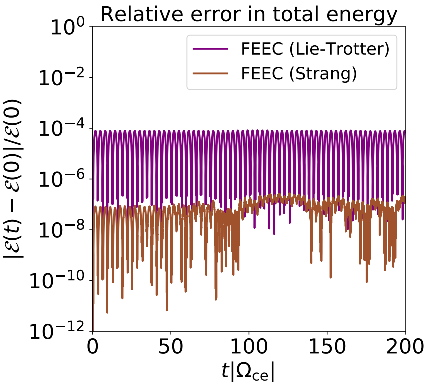

FEEC/GEMPIC: Results

Test run: Anisotropic Maxwellian ($\nu_\mathrm{h} = 6\%$, $v_{\mathrm{th}\|} < v_{\mathrm{th}\perp}$) for fast electrons and an initial magnetic field perturbation $\tilde{B}_x(z, t = 0) = a \sin(kz)$, **without** control variate

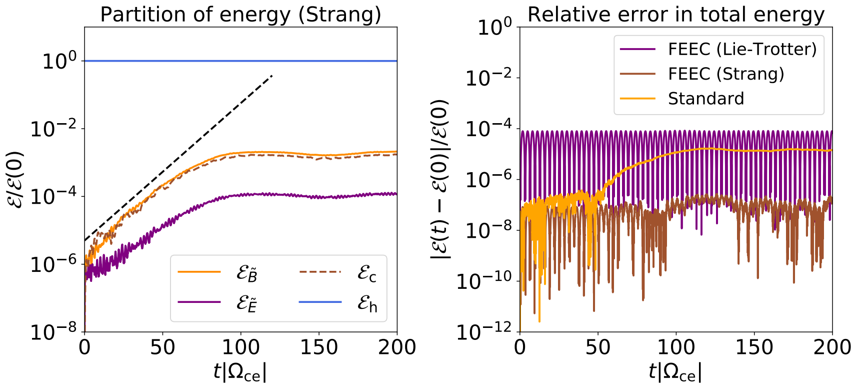

Outline

4. Summary

- Study of a high-frequency hybrid plasma model
  - cold fluid electrons
  - kinetic energetic electrons
- Anisotropic energetic electron distribution can drive instabilities
- Discretization of the model in two different ways:
  - Standard methods (B-spline finite elements + Boris particle pusher)
  - Geometric methods (Commuting diagram for function spaces, non-canonical Hamiltonian system, Hamiltonian splitting)
- Verification of codes by comparison with analytical dispersion relation
- Comparison of numerical schemes in terms of long-term energy conservation
  $\longrightarrow$**Similar in linear phase, geometric code better in nonlinear phase even for 1d in space model**

References

L. Chen, F. Zonca: *Physics of Alfvén waves and energetic particles in burning plasmas*, Rev. Mod. Phys. **88**, 015008 (2016).

X. Tao: *A numerical study of chorus generation and the related variation of wave intensity using the DAWN code*, J. Geophys. Res. Space Physics **119**, 3362-3372 (2014).

D. N. Arnold, R. S. Falk, R. Winther: *Finite Element exterior calculus, homological techniques, and applications*, Acta Numerica **15**, 1-155 (2006).

M. Kraus, K. Kormann, P. J. Morrison, E. Sonnendrücker: *GEMPIC: geometric electromagnetic particle-in-cell methods*, J. Plasma Phys. **83**, 905830401 (2015).

M. Brambilla: *Kinetic Theory of Plasma Waves: Homogeneous Plasmas*, Oxford University Press, Oxford, 1998.

A. Standard FEM/PIC: Convergence without control variate $\rightarrow$ with control variate

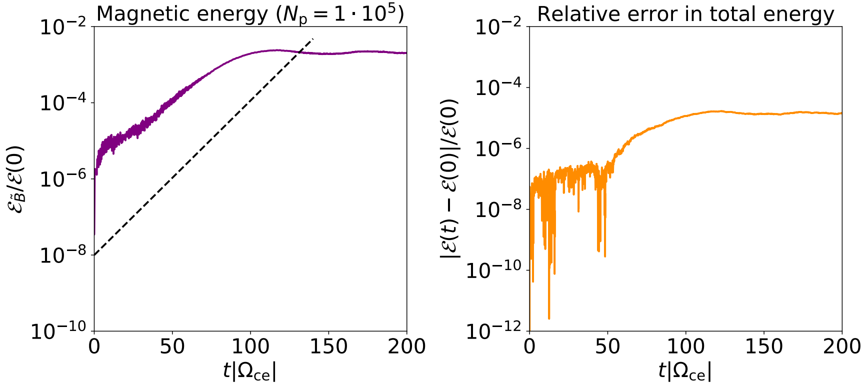

A. Standard FEM/PIC: Convergence without control variate → with control variate

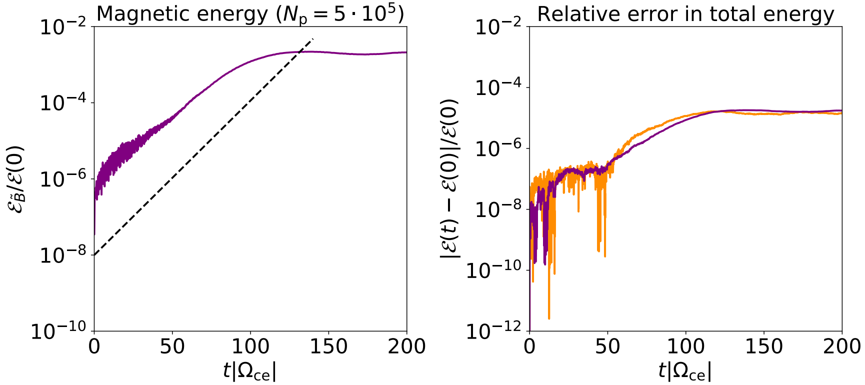

A. Standard FEM/PIC: Convergence without control variate $\rightarrow$ with control variate

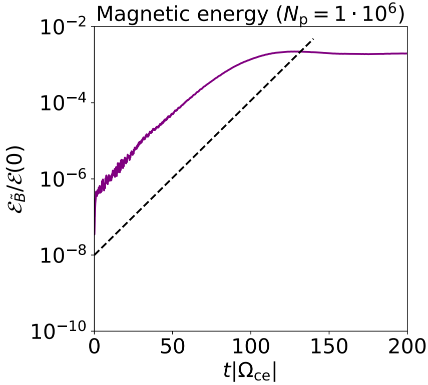

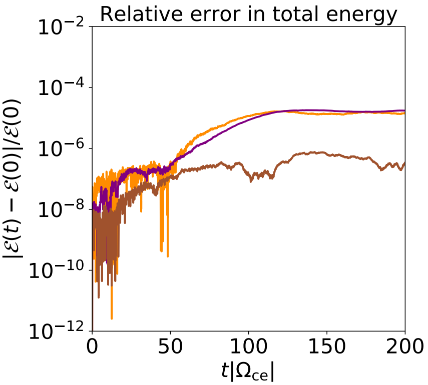

Supplementary material

A. Standard FEM/PIC: Convergence without control variate $\rightarrow$ with control variate

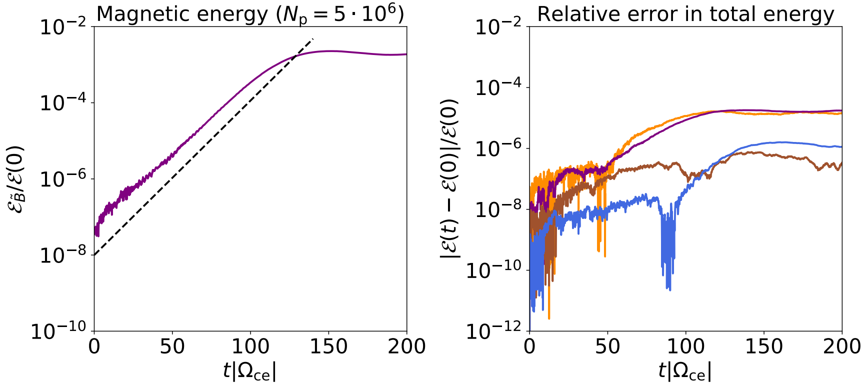

A. Standard FEM/PIC: Convergence without control variate $\rightarrow$ with control variate

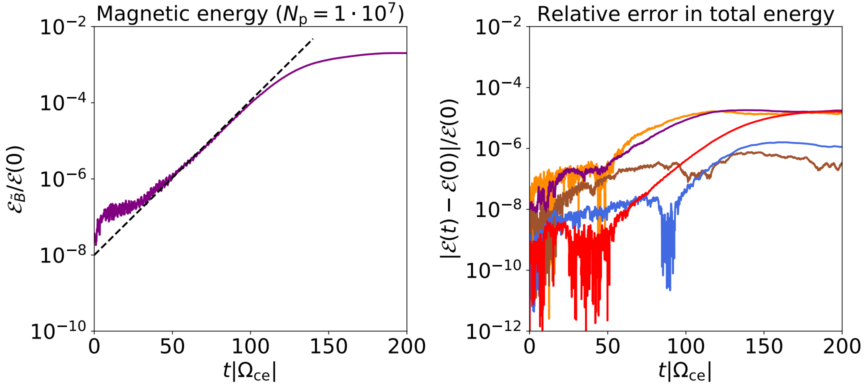

A. Standard FEM/PIC: Convergence without control variate → with control variate

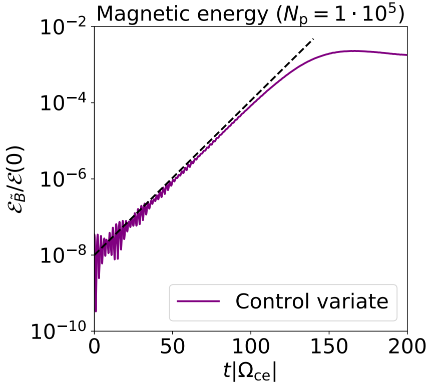

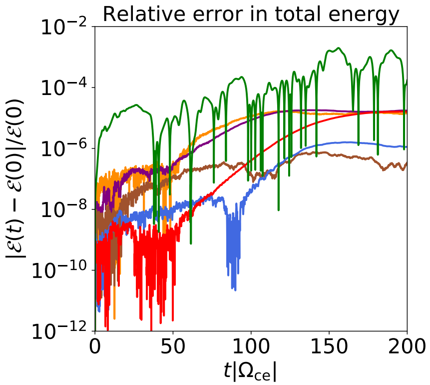

B. Standard finite elements/PIC: Excitation of multiple mode

Test run: Low density ($\nu_\mathrm{h} = 0.2\%$), isotropic Maxwellian ($v_{\mathrm{th}||} = v_{\mathrm{th}\perp}$) for fast electrons and no initial field perturbations, **with** control variate

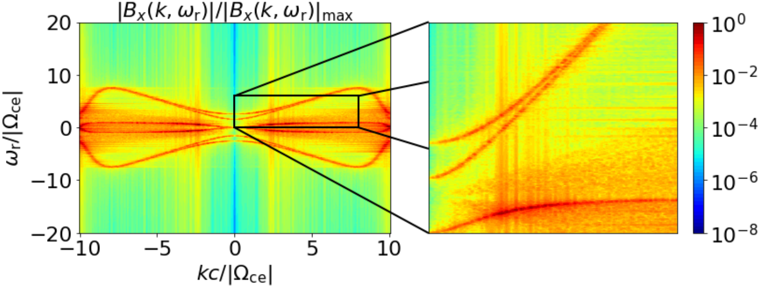

Figure: Spectrogram in k-ω_r-plane and comparison with dispersion relation

B. Standard finite elements/PIC: Excitation of multiple modes

Test run: Low density ($\nu_\mathrm{h} = 0.2\%$), isotropic Maxwellian ($v_{\mathrm{th}\|} = v_{\mathrm{th}\perp}$) for fast electrons and no initial field perturbations, **with** control variate

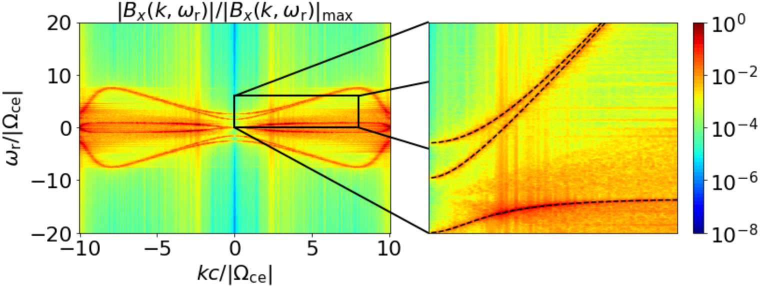

Figure: Spectrogram in k-ω_r-plane and comparison with dispersion relation

C. FEEC/GEMPIC: Impact of control variate

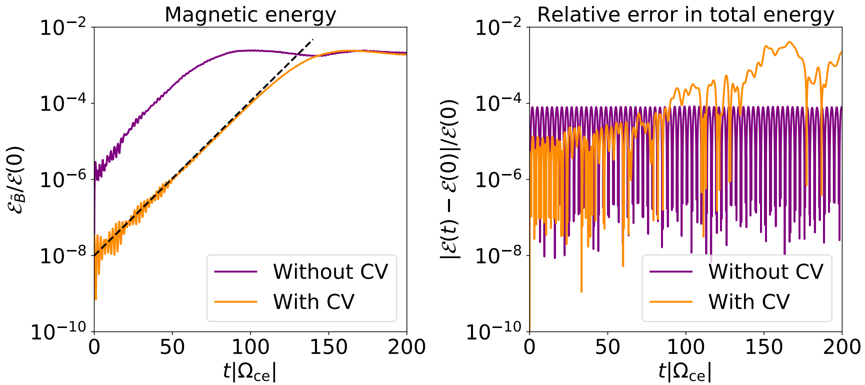

D. Standard FEM/PIC: Chorus waves

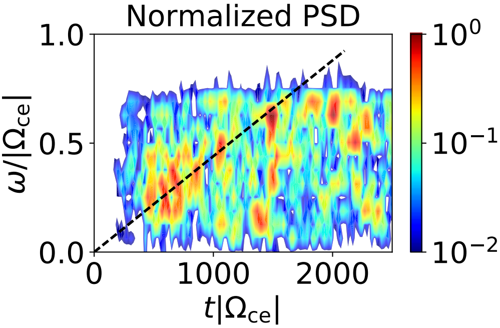

Figure: Power spectral density for a dipole-like background field